Pressure and Temperature Dependence of the Reaction of Vinyl Radical with Ethylene†

Huzeifa Ismail,‡ C. Franklin Goldsmith,§ Paul R. Abel,§ Pui-Teng Howe,|| Askar Fahr,*,⊥ Joshua B. Halpern,⊥ Leonard E. Jusinski,▽ Yuri Georgievskii,▽ Craig A. Taatjes,*,▽ and William H. Green*,§

Departments of Chemistry and Chemical Engineering, Massachusetts Institute of Technology, Cambridge, Massachusetts 02139, Department of Chemistry, American University, Washington, District of Columbia 20016, Department of Chemistry, Howard University, Washington, District Of Columbia, 20059, and Combustion Research Facility, Mail Stop 9055, Sandia National Laboratories, Livermore, California 94551-0969

Received: February 6, 2007; In Final Form: April 19, 2007

This work reports measurements of absolute rate coefficients and Rice−Ramsperger−Kassel−Marcus (RRKM) master equation simulations of the $C_2H_3 + C_2H_4$ reaction. Direct kinetic studies were performed over a temperature range of 300−700 K and pressures of 20 and 133 mbar. Vinyl radicals ($H_2C{=}CH$) were generated by laser photolysis of vinyl iodide (C_2H_3I) at 266 nm, and time-resolved absorption spectroscopy was used to probe vinyl radicals through absorption at 423.2 nm. Measurements at 20 mbar are in good agreement with previous determinations at higher temperature. A weighted three-parameter Arrhenius fit to the experimental rate constant at 133 mbar, with the temperature exponent fixed, gives $k = (7 \pm 1) \times 10^{-14}$ cm^3 molecule^{-1} s^{-1} $(T/298\ \text{K})^2$ exp[−(1430 ± 70) K/T]. RRKM master equation simulations, based on G3 calculations of stationary points on the C_4H_7 potential energy surface, were carried out to predict rate coefficients and product branching fractions. The predicted branching to 1-methylallyl product is relatively small under the conditions of the present experiments but increases as the pressure is lowered. Analysis of end products of 248 nm photolysis of vinyl iodide/ethylene mixtures at total pressures between 27 and 933 mbar provides no direct evidence for participation of 1-methylallyl.

Introduction

The reactions of hydrocarbons at high temperature are central to an understanding of combustion chemistry as well as petroleum processing. Vinyl radical ($H_2C{=}CH$) reactions play an important role in hydrocarbon pyrolysis and combustion processes.[1] Ethylene is the simplest olefin, hence its thermal chemistry serves as the basis for understanding the thermal chemistry of other olefins. At temperatures below 1000 K, C_2H_4 decomposition proceeds primarily through disproportionation to give C_2H_5 and C_2H_3.[2,3] Although the chemistry of C_2H_5 is fairly well understood, the chemistry of C_2H_3 remains relatively unexplored. For example, there have been few direct studies of the kinetics and product branching of the important C_2H_3 self-reaction,[4−8] although a number of studies have treated the combination/disproportionation channels of the vinyl self-reaction in models of complex reaction systems.[5,9−13]

An understanding of the $C_2H_3 + C_2H_4$ reaction system supports a more accurate description of C_2H_4 pyrolysis in particular and olefin pyrolysis in general. Moreover, polyethylene is one of the most important synthetic polymers. It is a widely used multipurpose material and has the largest annual production among all synthetic commodity polymers. In recent years, gas-phase polymerization has emerged as the most versatile process for the production of polyethylene. However, many fundamental microscopic processes involved in gas-phase ethylene polymerization are not completely understood.[14] The reaction between the vinyl radical and ethylene

$$C_2H_3 + C_2H_4 \xrightarrow{k_1} \text{products} \qquad (1)$$

has potential importance as the initiating and/or propagating step in gas-phase ethylene polymerization. Furthermore, it has been suggested[15,16] that reaction 1 may produce resonance-stabilized 1-methylallyl radicals, possible contributors to molecular weight growth in rich hydrocarbon flames.[17] Surprisingly, there has been only a limited number of studies on the $C_2H_3 + C_2H_4$ reaction to date.

Fahr and Stein[18] employed the very low pressure pyrolysis (VLPP) technique to study the kinetics and products of the $C_2H_3 + C_2H_4$ reaction over a temperature range of 1023−1273 K and at low pressure between 1.3 and 13 μbar. Temperature-dependent rate parameters for the $C_2H_3 + C_2H_4$ reaction were derived relative to the vinyl self-reaction, $C_2H_3 + C_2H_3$. More recently, Shestov et al.[16] reported kinetic studies of the $C_2H_3 + C_2H_4$ reaction from 625 to 950 K and at pressures between 7 and 15 mbar, using the laser photolysis/photoionization mass spectroscopy (LP/PIMS) technique. Under the conditions of these two previous studies, C_4H_6 and C_4H_7 were detected as the only major products. Both of the previous studies were done under conditions of low pressures and high temperature. The goal of the present study was to confirm the earlier results, extend them to lower temperature, and measure pressure dependence.

In the present work, the rate coefficient for the reaction of C_2H_3 with C_2H_4 has been measured over a temperature range

† Part of the special issue "M. C. Lin Festschrift".

* Authors to whom correspondence should be addressed. E-mail afahr@msrce.howard.edu (A.F.), cataatj@sandia.gov (C.A.T.), or whgreen@mit.edu (W.H.G.).

‡ Department of Chemistry, MIT.

§ Department of Chemical Engineering, MIT.

|| American University.

⊥ Howard University.

▽ Sandia National Laboratories.

10.1021/jp071041l CCC: $37.00
Published on Web 06/15/2007

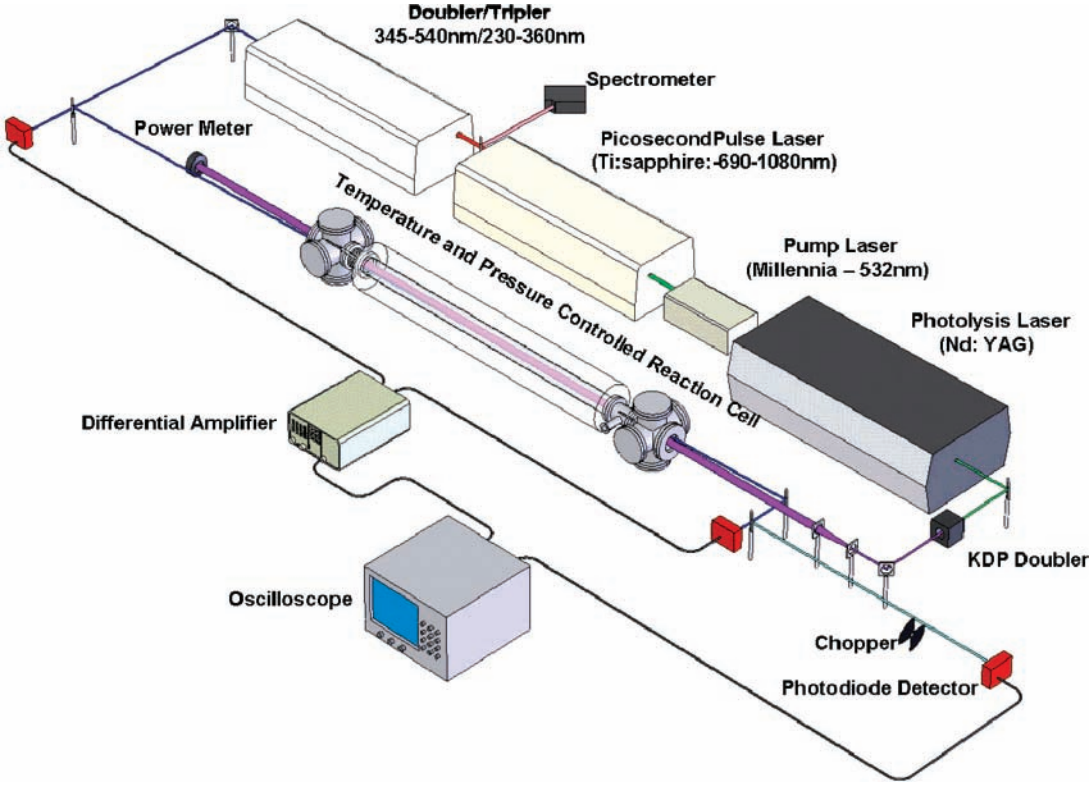

Figure 1. Diagram of experimental apparatus.

of 300−700 K and for pressures of 20 and 133 mbar. The reaction is modeled with Rice−Ramsperger−Kassel−Marcus (RRKM) master equation simulations, yielding pressure-dependent rate coefficients and branching fractions into primary products. The RRKM master equation simulations suggest that 1-methylallyl production decreases with increasing pressure and is a minor channel of reaction 1 under the conditions of the present study. End-product analysis of vinyl iodide/ethylene mixtures subjected to 248 nm photolysis between 27 and 933 mbar shows no direct evidence for 1-methylallyl formation.

Experimental Procedures

Kinetic Studies. Measurements of absolute total rate coefficients for the title reaction were performed in the Massachusetts Institute of Technology's Combustion Dynamics Laboratory. Vinyl radical (C_2H_3) was generated via laser photolysis of vinyl iodide at 266 nm:

$$C_2H_3I + h\nu\ (266\ \text{nm}) \rightarrow I + C_2H_3 \qquad (2)$$

Photolysis pulses were generated by frequency-doubling the 532 nm output of a short pulse Nd:YAG laser. The experimental apparatus is represented in Figure 1.

Direct absorption by vinyl radical was used to monitor the reaction of vinyl + ethylene. Vinyl radicals were detected by multiple-pass laser absorption at 423.3 nm.[19] The detection wavelength was generated by use of a mode-locked Ti:sapphire laser (1.2 ps at 80 MHz) pumped by a 532 nm diode-pumped solid-state continuous-wave (CW) laser. The output of the Ti:sapphire laser was frequency-doubled by use of a BBO crystal or frequency-converted by use of an OPO crystal producing an overall spectral range of 230−1200 nm.

The picosecond Ti:sapphire laser could easily be tuned through its entire spectral range, without any major changes to the optical path. This laser system has excellent stability on the microsecond-to-millisecond time scale, so it can be used as a quasi-CW source, allowing detection of transient absorbances as small as ~0.0001. A complete transient is measured following each photolysis pulse, making the measurement relatively insensitive to fluctuations in the photolysis laser output. A high-resolution spectrometer (0.1 nm fwhm) was used to determine the output wavelength. The fwhm resolution of the probe laser system in the present experiments is ~13 cm^{-1}. This resolution limits studies to molecules with broad absorption features. The spectrum of vinyl radical is ideal for such a probe laser, because its absorption features are broader than the laser fwhm yet still narrow enough to allow tuning off-resonance, as shown in Figure 2. The off-resonance signal contains contributions from thermal lensing noise; the vinyl concentration is taken to be proportional to the difference in absorption between traces taken on- and off-resonance.

The experiment was carried out in a 160 cm long temperature-controlled stainless steel flow reactor. An internally mounted Herriott-type multiple-pass cell provides an overall probe path

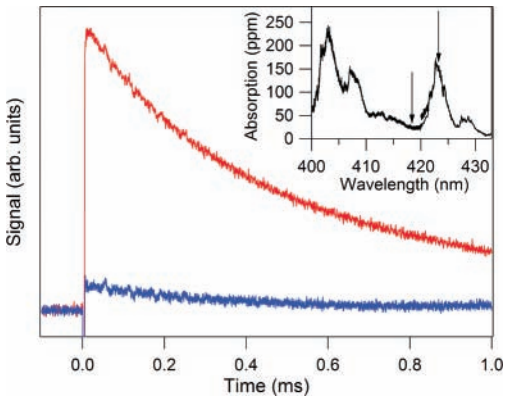

Figure 2. (Red trace) On-resonance of C_2H_3 at 423.2 nm; (blue trace) off-resonance taken at 418.0 nm. (Inset) Section of the vinyl radical absorption spectrum as reported by Shahu et al.,[19] with the probe wavelengths of the two traces shown by vertical arrows.

length of up to 40 m, allowing detection of transient absorptions with [absorption cross section × concentration] products less than 10^{-7} cm^{-1}. To improve the signal-to-noise ratio, a balanced detection scheme was used where a reference beam (I_0) that does not pass through the reactor is normalized to and subtracted from the probe beam (I) by use of a continuously variable optical attenuator and a low-noise differential amplifier.

Calibrated mass flow controllers were used to maintain a constant flow of the reactant and buffer gases. Flows are sufficient to completely refresh the cell every 4−5 shots at the 1 Hz repetition rate of the photolysis laser. A very small portion of the photolyte (∼0.2%) in the path of the laser is dissociated on each pulse, and the photolysis laser intersects less than about 20% of the total cell volume. Varying the laser repetition rate over a factor of 50 (between 0.1 and 5 Hz) produced no systematic change in the observed decay rate. The internal pressure of the reactor is measured by a capacitance manometer and controlled with an automated butterfly valve. Both the flow controllers and automatic butterfly valve were set and adjusted via computer interface. The flow reactor was housed in a cylindrical oven. Additional resistive heating was supplied to the reactor entrance and exit region. The entrance, center, and exit temperatures were monitored with K-type thermocouples, which were fed into three independent PID controllers to maintain a constant temperature. Direct measurements of the temperature profile along the center axis of the reactor confirmed that the temperature in the interaction zone varied by less than ∼2% at the highest temperatures of this study.

The kinetics experiments were performed between 300 and 700 K at high pressure (133 mbar) and between 500 and 700 K at low pressure (20 mbar). To maintain pseudo-first-order conditions, ethylene concentrations (5×10^{16} to 8×10^{17} cm^{-3}) were in large excess over vinyl (∼2×10^{12} cm^{-3}), also ensuring that the pseudo-first-order decays were at least 5 times faster than the decay without added ethylene. For most of the experiments, vinyl iodide concentrations were maintained at [C_2H_3I] = 1×10^{15} cm^{-3}. Some experiments were performed at several concentrations of vinyl by varying photolysis laser intensity and C_2H_3I concentration. It was found that the rate constants did not depend on [C_2H_3] or on photolysis energy, confirming the validity of a pseudo-first-order approximation and suggesting a negligible role for photolytic interferences.

Although dissociation of ethylene has been reported in other experiments from irradiation at 248 nm,[16] no photolysis of ethylene at 266 nm was observed in the present experiments, and no transient absorption of the 423.2 nm probe laser could be detected from 266 nm irradiation of pure ethylene, even at 130 mbar and 700 K. Excitation at 266 nm is near or below the origin of the first singlet excitation in ethylene, and the only absorption is expected to be in the extremely weak first triplet band.[20] Furthermore, the 107.5 kcal mol^{-1} energy of a 266 nm photon (7.8 kcal mol^{-1} less energy than a 248 nm photon) is less than the C−H bond energy in ethylene [D_0 = (109.7 ± 0.8) kcal mol^{-1}].[21]

To determine k_1, the decay rate of C_2H_3 was measured as a function of the ethylene concentration [C_2H_4]. Values of k_1 were obtained in the usual manner as the slope of a plot of the pseudo-first-order rate constant for vinyl loss, k' (where $k' = k_1[C_2H_4] + k_2$), versus [C_2H_4]. The effective rate constant k_2, represented by the zero-ethylene intercept of this plot, is attributable to all other loss processes for vinyl radical, including self-reaction and reaction with the photolytic precursor, diffusion out of the beam, and heterogeneous loss. Plotting k' versus [C_2H_4] yielded

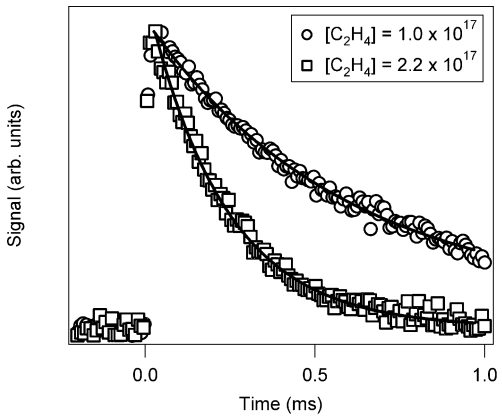

Figure 3. Recorded decay of C_2H_3 at 550 K and 133 mbar for the conditions [C_2H_4] = 1×10^{17} cm^{-3} (○) and [C_2H_4] = 2.2×10^{17} cm^{-3} (□). Every 100th point is shown for clarity. Single-exponential fits are shown as solid lines.

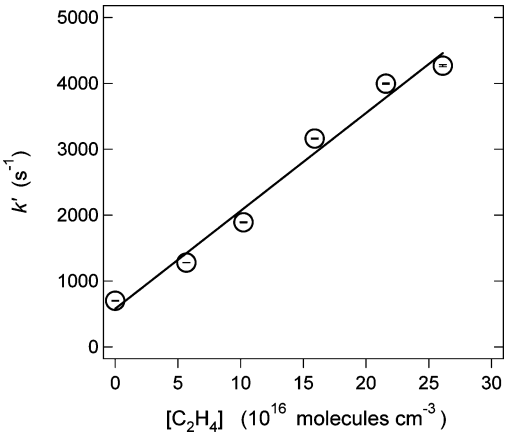

Figure 4. Pseudo-first-order C_2H_3 decay rate k' vs [C_2H_4], at a temperature of 550 K and a total density of 2.6×10^{17} cm^{-3} (20 mbar pressure).

lines of constant slope as shown in Figure 4. The uncertainty limits of k' shown in Figure 4 represent the statistical uncertainty resulting from the fit of the C_2H_3 decay data to a single exponential. Ethylene concentrations used were large enough that the error in simply including the second-order contribution from self-reaction in the intercept was small. Extracting k' from the first-order component of a fit to the functional form for a combined first- and second-order decay resulted in identical values of k_1 within experimental uncertainty.

Modeling Methods. The kinetics of reaction 1 were modeled by using a RRKM master equation approach, employing the VariFlex[22] program package. The optimized geometries and zero-point corrected energies for the C_4H_7 isomers and the transition states calculated by Miller[15] were used as the starting point. The simplified potential energy surface for the vinyl + ethylene reaction was similar to that employed by Shestov et al.[16] and includes the 3-buten-1-yl, 1-methylallyl, and 1-buten-1-yl isomers of the C_4H_7 radical as well as the vinyl + ethylene and H + (*cis*-, *trans*-) 1,3-butadiene bimolecular channels, as shown in Figure 5. Unlike the potential energy surface employed by Shestov et al., two transition states are provided for the isomerization between 3-buten-1-yl and 1-methylallyl: *cis*-3-buten-1-yl to *cis*-1-methylallyl and *trans*-3-buten-1-yl to *trans*-1-methylallyl. With the exception of these two explicit transition states, the contributions of the cis and trans conformers of the C_4H_7 species are included in an approximate fashion by treating the cis−trans isomerization as a hindered internal rotor and compensating the effective symmetry numbers in the RRKM

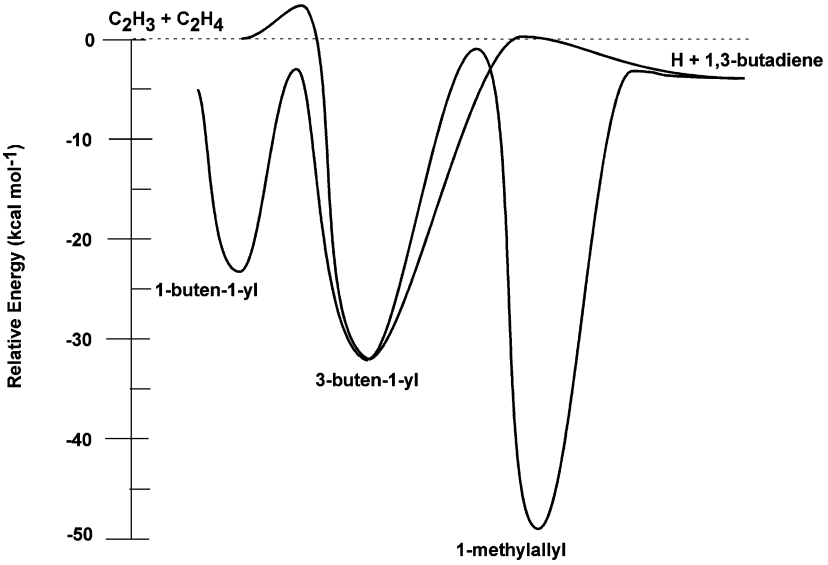

Figure 5. Schematic potential energy surface for the reaction of vinyl with ethylene. Two transition states (cis and trans) for isomerization of 3-buten-1-yl to 1-methylallyl are included in the master equation calculations; only one is shown.

calculations. A single-exponential down model was used for the energy transfer, with an average ΔE_{down} given by 350 cm^{-1} $(T/298)$,$^{0.8}$ from analogy with other reactions.[23,24] As very little falloff is observed in the predicted total rate coefficient, the dependence of k_1 on the choice of ΔE_{down} is minuscule. The effect on branching fraction is more substantial, in accord with what would be predicted from the pressure dependence. The Supporting Information contains master equation solutions for a range of energy transfer parameters.

The Miller[15] calculations used G3//B3LYP for most stationary points but used G3 for the loose transition states in the entrance and exit channels. For consistency, in the present calculations all stationary points have been recalculated by G3 methods[25] with the Gaussian 03 package.[26] As the relatively loose bond-fission transition states (the entrance barrier transition state and the transition state between 1-methylallyl and H + 1,3-butadiene) are most likely to exhibit multireference character, they were also calculated by CASPT2(5e,5o)/aug-cc-pVDZ methods. However, the final master equation solutions differed little from those carried out with the G3 results, and the G3 stationary points are used in all the results reported here. Computed geometries, frequencies, and energies for all stationary points are given in the Supporting Information. Additional quantum calculations for hindered rotations were calculated at the B3LYP/6-311G(d,p) level with Gaussian 03.[26] Each hindered rotor was treated as a one-dimensional hindered rotor (with a Pitzer−Gwinn[27]-like approximation that

$$Q = \frac{Q_{\text{classical hindered rotor}} Q_{\text{quantum harmonic oscillator}}}{Q_{\text{classical harmonic oscillator}}}$$

with barriers to hindered internal rotation fit to Fourier series. Tunneling was included for all transition states by use of an Eckart barrier model, where the parameters for the Eckart expression are computed from the barrier heights and the imaginary frequency at the transition state. Because the tunneling correction is minor, more detailed procedures, such as fitting of the potential near the barrier,[28] were deemed unnecessary.

Because of the substantial secondary chemistry in the end-product experiments, a comprehensive mechanism is desirable for even qualitative interpretation. The reaction mechanism for the product analysis was generated by use of RMG 2.0, an open-source automatic reaction model generating program.[29] The algorithm for mechanism generation has been described in detail previously.[29,30] In brief, the complete reaction system (subject to some tolerance parameter) is calculated, with rate constants for all possible reactions between the available species estimated on the basis of rules for classes of reactions. Thus a model is generated that is comprehensive (in the sense that it includes all relevant reactions), albeit with approximate rate coefficients. Thermodynamic parameters and high-pressure-limit rate parameters are stored in a hierarchical database based on functional groups. Thermodynamic parameters for specific molecules are included in a primary thermodynamic library, and thermodynamic properties for all other molecules are estimated by group additivity. RMG's kinetics database is divided into 34 reaction families. Small molecule reactions that cannot be described by reaction families are included in a primary reaction library. The temperature, pressure, and initial concentrations of vinyl radical, ethylene, and helium were provided to RMG as input; it was assumed that 1% of the initial vinyl iodide is photolyzed to form the vinyl radical. By default, this version of RMG uses the high-pressure limit values when estimating unknown rate constants by reaction-family rules. The rate constants pertaining to the vinyl + ethylene potential energy surface were added as a reaction library, replacing the RMG-estimated high-pressure rate constant with the pressure-dependent rate constants generated from the master equation calculations. This process was repeated for 523, 623, and 723 K and for 27, 200, 533, and 933 mbar, thereby yielding 12 mechanisms. The Supporting Information contains the mechanism used for 523 K and 533 mbar.

End-Product Studies. In order to determine the products of the vinyl + ethylene reaction, final stable gas-phase products were characterized from vinyl iodide/ethylene mixtures subjected to 248 nm photolysis. Final products from subsequent reaction of 3-buten-1-yl and 1-methylallyl should be distinguishable. Unfortunately, because of the extensive chain reactions in this system (resulting in substantial carbonaceous deposits in the reaction cell), the mole balance between the reactant depletion and the gas-phase products was poor (about 50%), and only qualitative conclusions regarding the role of 1-methylallyl can be drawn from the product measurements. The experimental

TABLE 1: Conditions and Results of Experiments To Measure k_1

T (K)	P (mbar)	$[C_2H_3I]$ (10^{15} cm^{-3})	$[C_2H_3]_0$[a] (10^{12} cm^{-3})	$[C_2H_4]$ (10^{17} cm^{-3})	k_1[b] (10^{-15} cm^3 molecule^{-1} s^{-1})	k_2[c] (s^{-1})
298	133	1.30	3.90	4.0−33.0	0.60 ± 0.06	816
325	133	1.16	3.20	3.0−30.0	0.99 ± 0.05	636
350	133	1.32	3.80	2.0−7.5	2.3 ± 0.3	926
375	133	1.23	3.44	1.2−7.0	3.1 ± 0.3	826
400	133	1.15	2.50	1.1−6.5	3.6 ± 0.4	913
425	133	1.08	2.24	1.0−6.1	4.7 ± 0.6	900
450	133	1.02	2.11	0.9−4.8	7.0 ± 0.6	672
475	133	1.06	2.81	0.9−4.6	9.6 ± 0.6	701
500	133	1.01	2.14	0.9−4.3	11.7 ± 0.7	557
525	133	0.96	1.81	0.8−4.0	14.0 ± 0.4	430
550	133	1.04	2.20	0.8−3.9	19.0 ± 1.2	347
575	133	1.03	3.70	0.8−3.8	23 ± 2	279
600	133	1.06	2.15	0.7−3.7	22.4 ± 2	901
625	133	1.09	1.90	0.7−3.5	27.6 ± 2.8	846
650	133	1.05	1.60	0.6−3.4	44 ± 4	280
675	133	1.05	2.62	0.4−2.3	43 ± 3	784
700	133	1.05	3.37	0.2−1.8	54 ± 3	339
500	20	1.06	2.51	1.0−2.9	9.1 ± 0.9	763
550	20	1.04	2.04	0.6−2.6	14.9 ± 1.0	582
600	20	1.05	1.90	0.5−2.4	19 ± 1	894
650	20	1.05	1.89	0.4−2.2	28 ± 3	808
700	20	1.03	1.75	0.2−2.0	40 ± 4	839

[a] Determined from a C_2H_3 cross section of 2×10^{-19} cm^2.[36] [b] Uncertainty limits ($\pm 1\sigma$) based on statistical uncertainties in the fits. [c] y-Intercept of the plot of pseudo-first-order rate constant vs ethylene concentration.

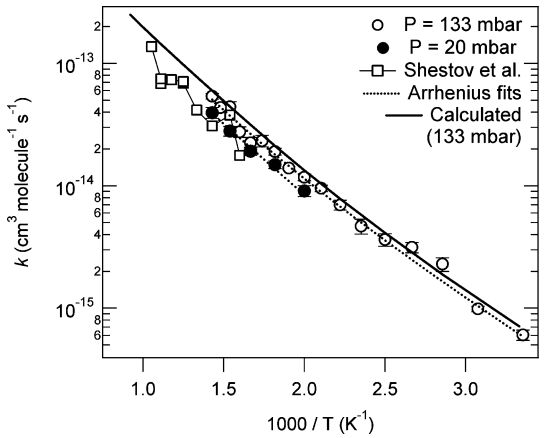

Figure 6. Temperature dependence of the total rate constant for reaction of vinyl with ethylene: (O) experimental results of the present study at 133 mbar; (●) experimental results of the present study at 20 mbar; (□) results reported by Shestov et al.[16] (···) Arrhenius fits for each of the two present data sets;(−) master equation calculations (133 mbar).

methods have been described elsewhere,[31] hence only a brief description will be given here.

Vinyl radicals were generated from 248 nm excimer laser photolysis of vinyl iodide (C_2H_3I). Dilute mixtures of C_2H_3I (7×10^{13} to 3×10^{15} cm^{-3}) and C_2H_4 (7×10^{15} to 3×10^{17} cm^{-3}) in He (27−933 mbar) were irradiated in a cylindrical temperature-controlled quartz reaction cell (10 cm long, with 2 cm inner diameter). The photolyzed reaction mixture was circulated in an enclosed loop with a self-enclosed pump, which reduces but does not completely eliminate photolysis of products. The active photolysis volume was about 0.3% of the total volume of the loop. Photolysis times were typically 15 min at a repetition rate of 1 Hz or 30 min at a repetition rate of 0.5 Hz. The laser energy was typically 200 mJ/pulse as measured at the source. Under these conditions, the C_2H_3 radical concentrations generated from photolysis typically range from 6×10^{11} to 3×10^{13} cm^{-3}. These radical concentrations were determined from gas chromatographic measurements of the C_2H_3I loss due to photolysis.

The product analysis studies were carried out at temperatures of 523, 623, and 723 K, for pressures ranging from 27 to 933 mbar. Ethylene undergoes slight photolysis (1−2%) at temperatures above 623 K. The principal products of ethylene photochemistry at 248 nm are 1-butene and 1,3-butadiene. Experiments were performed where ethylene was irradiated in the reaction cell in the absence of vinyl iodide in order to account for ethylene photolysis. Similarly, the contributions to the products from C_2H_3I pyrolysis and photolysis were assessed through a number of control experiments in which vinyl iodide/He samples were irradiated in the absence of ethylene or kept in the heated reaction cell without irradiation.

Reaction products were separated, identified, and quantified by use of an on-line gas chromatography/mass spectroscopy (GC/MS) system, interfaced with a flame ionization detector (FID) and a quadrupole mass spectrometer. Calibration of retention times, response factors, and comparison of cracking patterns with known standard samples enabled positive identification and quantification of the products. However, as noted above, secondary chemistry precludes quantitatively relating the observed products to primary branching fractions in the vinyl + ethylene reaction.

Results and Discussion

Kinetic Measurements. The measured values for k_1 are given in Table 1, and an Arrhenius plot of k_1 is shown in Figure 6. A simple Arrhenius fit to the measured rate coefficient for reaction 1 at 133 mbar, weighted by the uncertainties in the individual data points, yields

$$k_1 = (1.2 \pm 0.2) \times 10^{-12}\ \text{cm}^3\ \text{molecule}^{-1}\ \text{s}^{-1} \exp[-(2310 \pm 70)\ \text{K}/T] \quad (3)$$

and a similar fit to the present results at 20 mbar gives

$$k_1 = 8.8 \times 10^{-13}\ \text{cm}^3\ \text{molecule}^{-1}\ \text{s}^{-1} \exp[-2330\ \text{K}/T] \quad (4)$$

where the limited number of determinations at 20 mbar does not permit useful uncertainty analysis of the fitting parameters. The error limits in the Arrhenius expression (eq 3) are the 95%

TABLE 2: Comparison of Vinyl + Ethylene Rate Constants from Literature and This Study

source	method	temp range (K)	pressure (mbar)	*A*-factor (cm^3 $molecule^{-1}$ s^{-1})	E_a/R (K)
ref 32	thermochemical estimate	1170−1430		8.3×10^{-13}	0
ref 18	very low pressure pyrolysis (VLPP)	1023−1273	0.0013−0.013	1.04×10^{-12}	1560
ref 15	computational quantum chemistry				1810[a]
ref 16	laser photolysis/photoionization mass spectrometry	625−950		2.04×10^{-12}	2830 ± 790
this study	laser photolysis/laser absorption	300−700	133	$(1.2 \pm 0.2) \times 10^{-12}$	2310 ± 70
		500−700	20	8.8×10^{-13}	2330

[a] Relative enthalpy of transition state on potential energy surface.

uncertainty in the fit parameters, weighted by the precision in the individual rate constants determined from the linear fit of the k' data to an exponential. A better fit to the observed data at 133 mbar is given by a modified Arrhenius form, with the temperature exponent fixed at 2:

$$k_1 = (7 \pm 1) \times 10^{-14}\ \mathrm{cm^3\ molecule^{-1}\ s^{-1}}\ (T/298\ \mathrm{K})^2 \times \exp[-(1430 \pm 70)\ \mathrm{K}/T] \quad (5)$$

This is the fit shown in Figure 6.

The reaction of vinyl radical with ethylene has been investigated previously by several authors. The results from all these studies have been summarized in Table 2. The previous experiments were generally carried out at conditions of lower pressure and higher temperature than the present experiments. Benson and Haugen[32] indirectly determined the rate constant for reaction 1 between 1100 and 1430 K via kinetic modeling of the ethylene pyrolysis study performed by Skinner and Sokoloski.[33] This rate coefficient is approximately a factor of 3−4 higher than an extrapolation of the Arrhenius fits to the results from many of the recent studies, including the present work. Fahr and Stein[18] determined the rate constant for reaction 1 for the temperature range 1023−1273 K relative to the vinyl radical recombination to form butadiene. By use of an assumed rate constant for the butadiene-forming channel of the vinyl recombination of 3.3×10^{-11} cm^3 $molecule^{-1}$ s^{-1}, their derived k_1 values are in reasonable agreement with an extrapolation of the Arrhenius fit reported by Shestov et al.[16]

The activation energy from an Arrhenius fit to the present data taken at 133 mbar is found to be (4.6 ± 0.2) kcal mol^{-1}. This activation energy is approximately 1 kcal mol^{-1} lower than the activation energy obtained from an Arrhenius fit to the data of Shestov et al.[16] and ∼1 kcal mol^{-1} greater than the entrance barrier calculated by Miller.[15] Shestov et al.[16] found that raising the energy for the entrance transition state from Miller's value by 1.3 kcal mol^{-1} gave good agreement of their master equation calculations with the experimental data. This correction is within the accuracy of the G3//B3LYP method used by Miller.[15] As shown in Figure 6, the present master equation calculations fit the 133 mbar data reasonably well without modification to the G3 energies. The present data at 20 mbar agree with the data of Shestov et al.,[16] whereas the rate coefficient at 133 mbar appears consistently ∼20−30% higher at all temperatures, suggesting the vinyl + ethylene reaction is in the falloff region at the present experimental conditions and those of Shestov et al. The master equations predict a very slight falloff, as shown in Figure 7, with k_1(20 mbar) ∼20% smaller than k_1(133 mbar) at 700 K.

One of the intriguing aspects of the vinyl + ethene reaction in the context of molecular weight growth and soot formation in combustion is the possibility of forming resonance-stabilized C_4H_7 radicals. Resonance-stabilized radicals are less reactive than their unstabilized isomeric counterparts and tend to reach larger concentrations in flames. As a result, resonance-stabilized radicals, in particular the propargyl (C_3H_3) radical, play a prominent role in aromatic formation and soot production. Miller[15] predicted formation of delocalized 1-methylallyl isomer in the vinyl + ethylene reaction. Shestov et al.[16] concluded from the thermal stability of the observed C_4H_7 product that substantial 1-methylallyl formation occurs in the reaction, and their master equation simulations suggested 40% of the reaction proceeded by this pathway under the low-pressure (total densities of 6×10^{16} cm^{-3}) conditions of their experiments. The present master equation calculations predict 1-methylallyl yields that (in general) rise with temperature and fall with increasing pressure, as shown in Figure 8.

An attempt was made to directly observe 1-methylallyl radical in the laser absorption experiments. Tonokura and Koshi[34] found allyl radical absorption to be in the same region as vinyl (370−420 nm). It is to be expected that 1-methylallyl would also have absorption bands in this region, except that it may be more diffuse. Under the conditions of high temperature (650 K), low pressure (20 mbar), and high ethylene concentration, a low-resolution spectrum of this system was taken from 390 to 440 nm. However, no features appeared that could be attributed to absorption by a 1-methylallyl reaction product. The visible absorption cross sections of vinyl radical and allyl radical are similar,[34−36] and the signal-to-noise ratio for the vinyl radical under these conditions is >20. However, the master equation simulations predict a relatively small yield of 1-methylallyl under these conditions, and it is possible that a 1-methylallyl yield consistent with the calculations simply is too small to be observed. Higher sensitivity measurements, possibly in other wavelength regions, may be required to observe absorption from 1-methylallyl produced in this reaction.

At temperatures below 500 K, the reaction between vinyl radical and ethylene predominantly forms the 3-buten-1-yl radical adduct, and the rate of 1-methylallyl formation is nearly negligible. As shown in Figure 8, the calculated production of 1-methylallyl formation at higher temperatures is strongly dependent upon the pressure; at 20 mbar, 1-methylallyl becomes significant for temperatures between 650 and 900 K, whereas

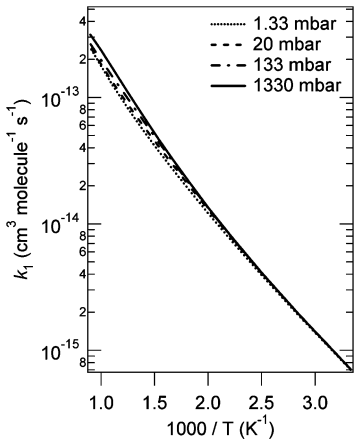

Figure 7. Master equation calculations of the total rate coefficient for vinyl reacting with ethylene at several pressures.

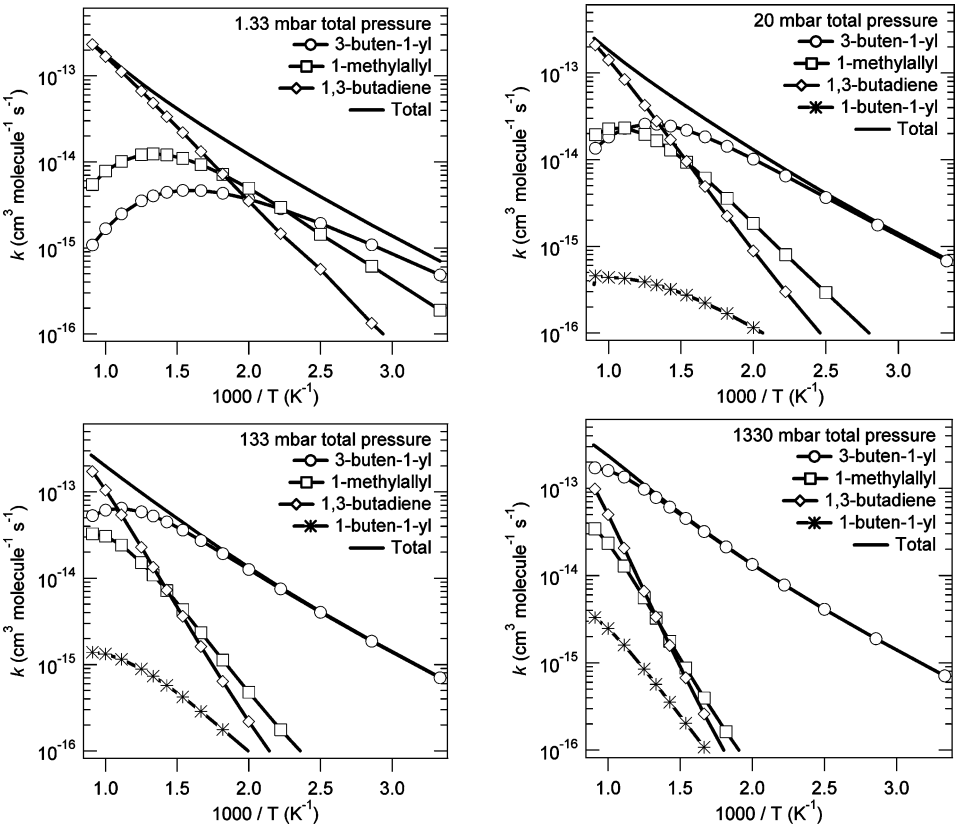

Figure 8. Master equation predictions for the product branching of the reaction between vinyl radical and ethylene at (upper left) 1.33 mbar, (upper right) 20 mbar, (lower left) 133 mbar, and (lower right) 1330 mbar.

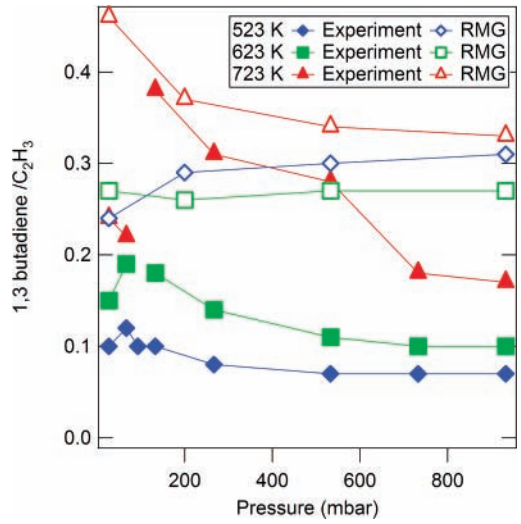

Figure 9. Experimental and RMG predicted yield of 1,3-butadiene versus total pressure.

at 133 mbar, the channel is predicted to be significant for temperatures between 800 and 1000 K. At still higher temperatures, the vinyl + ethylene reaction proceeds directly to the bimolecular products H + 1,3-butadiene via a chemically activated channel, and the yield of stabilized C_4H_7 is predicted to be very small. It should be noted that the stabilized 3-buten-1-yl radicals initially formed in the reaction may subsequently suffer thermal redissociation or (H-atom assisted) isomerization. Nevertheless, given the steep decrease in 1-methylallyl yields as the pressure increases, the vinyl + ethylene reaction appears unlikely to be an important source of resonance-stabilized radicals in realistic combustion systems.

Product Investigations. Earlier studies[16,18] identified C_4H_7 and H + C_4H_6 as the only products of the C_2H_3 + C_2H_4 reaction. The subsequent reactions of different C_4H_7 isomers should produce distinguishable end products. In the 248 nm photolysis of vinyl iodide/ethylene mixtures, the primary products suffer secondary reactions before the stable final products are detected. Acetylene, 1,3-butadiene, 1-butene, 1,5-hexadiene, cyclohexene, and 1,7-octadiene have been identified as end products. In addition, an unidentified product of molecular weight 82 was detected. It is likely that the products 1-butene, 1,5-hexadiene, cyclohexene, and the unidentified mass 82 product are formed mainly from the reactions of C_4H_7 radicals. The rule-based estimates in the RMG model predict the secondary chemistry based on families of known reactions, and the RMG mechanism therefore provides a framework for interpreting the observed stable products of the complex reaction system following 248 nm photolysis of vinyl iodide/ethylene mixtures. The RMG-generated mechanisms consisted of 114 species and ~7500 reactions.

The RMG model predicts a molar balance roughly similar to that observed in the experiments, suggesting that the overall loss to secondary chemistry is approximately consistent with known hydrocarbon chemistry. However, the quantitative agreement for the major products is relatively poor, as seen in Figure 9 for 1,3-butadiene. The full set of measured and predicted yields is available in the Supporting Information. In view of the disappointing quantitative predictions, inferences from comparisons of the model and the end product measurements are limited to qualitative information regarding relative yields.

The formation of 1-butene may arise from reactions of vinyl or H with either C_4H_7 isomer. Production of 2-butene, not experimentally observed, would also be expected from reactions of 1-methylallyl; the RMG model predicts 2-butene at about

$^1/_{10}$ the level of 1-butene. The C_4H_7 radicals predicted to be products of the reaction of vinyl with ethylene will yield various C_6H_{10} isomers from reactions with vinyl or with ethylene and isomers of C_8H_{14} from recombination reactions. For example, the observed 1,5-hexadiene is likely a product of the 3-buten-1-yl radical reacting with vinyl or ethylene. Cyclohexene is another likely product of the reaction of 3-buten-1-yl with ethylene. The 5-hexen-1-yl radical initially formed by the addition of 3-buten-1-yl to ethylene rapidly cyclizes,[37] and formation of cyclohexene + H is predicted to be facile.[38] Production of cyclohexene from 1-methylallyl seems rather less likely. Formation of cyclohexene + H in the reaction of 3-buten-1-yl with ethylene should be accompanied by a similar but smaller production of methylenecyclopentane + H.[39] The dependence of the unidentified mass 82 product on total pressure and ethylene partial pressure is similar to that of cyclohexene, and methylenecyclopentane is a likely source of the unidentified signal. Other isomers of C_6H_{10}, 1,4-hexadiene and 3-methyl-1,4-pentadiene, would be expected to arise, in approximately equal quantities, from 1-methylallyl reactions with vinyl (formation of H + linear C_6H_{10} isomers is substantially endothermic from 1-methylallyl + ethene). These isomers are not observed in the experiments; if one of them were responsible for the unidentified signal, a second unidentified mass 82 peak would be expected, corresponding to products of vinyl addition to the other radical site on 1-methylallyl.

Similarly, in addition to the above major reaction products, a small quantity of 1,7-octadiene was also observed, which most likely is produced through 3-buten-1-yl self-reaction. Recombination reactions of the 1-methylallyl radicals might be expected to be a more prominent loss pathway than for the 3-buten-1-yl radical because the resonance stabilization makes 1-methylallyl less reactive with stable molecules. The RMG mechanism predicts other C_8H_{14} isomers, such as 2,6-octadiene, that may be expected to result from recombination reactions of the 1-methylallyl radical or reactions of 1-methylallyl with 3-buten-1-yl, in concentrations similar to that of 1,7-octadiene. However, these isomers remain unobserved experimentally.

In conclusion, the observed products from the photolysis system can be rationalized as arising from secondary reactions of the primary 3-buten-1-yl and 1,3-butadiene products. With the possible but unlikely exception of the unassigned mass 82 product, stable species predicted to arise from the 1-methylallyl isomer have not been observed. Attempted in situ laser absorption detection of the 1-methylallyl product was also unsuccessful. Shestov et al.[16] directly observed C_4H_7 radicals by photoionization mass spectrometry, and their master equation calculations, as well as those reported here, predict larger 1-methylallyl production at the lower pressures of their experiments. Perhaps similar measurements with tunable photoionization[40] could be used to experimentally determine the relative importance of the C_4H_7 isomers.

Conclusions

The reaction kinetics and product channels of the $C_2H_3 + C_2H_4$ reaction have been studied at temperatures ranging from 300 to 723 K and over a pressure range of 27−933 mbar. A fit of the present measurements for this reaction at 133 mbar to a three-parameter Arrhenius form with a fixed temperature exponent yields

$$k_1 = (7 \pm 1) \times 10^{-14}\ \mathrm{cm^3\ molecule^{-1}\ s^{-1}}\ (T/298\ \mathrm{K})^2 \times \exp[-(1430 \pm 70)\ \mathrm{K}/T] \quad (5)$$

and a simple Arrhenius fit at 20 mbar yields

$$k_1 = 8.8 \times 10^{-13}\ \mathrm{cm^3\ molecule^{-1}\ s^{-1}}\ \exp(-2330\ \mathrm{K}/T) \quad (4)$$

The present results at 20 mbar agree with results of Shestov et al.,[16] and extrapolation of these data sets agrees well with the data of Fahr and Stein.[18] The rate constant measured at 133 mbar is consistently slightly higher than both the rate constant at 20 mbar and the data of Shestov et al., suggesting the vinyl + ethylene reaction is in the falloff region in the present work and at the lower pressure conditions of Fahr and Stein and Shestov et al.'s studies. Master equation calculations based on G3 characterization of stationary points on the C_4H_7 surface give good agreement with the magnitude of the observed rate coefficients at 133 mbar but may slightly underestimate the falloff in the total rate coefficient.

Acknowledgment. This work was supported by the Division of Chemical Sciences, Geosciences, and Biosciences, Office of Basic Energy Sciences (BES), U.S. Department of Energy (DOE). Part of the work of A.F. and P.-T. H. was supported by DOE/BES Contract DE-FG02-02ER15360. The work at MIT was funded by DOE/BES under Contract DE-FG02-98ER14914. C.F.G. acknowledges fellowship support from the Department of Defense. Helpful comments and suggestions on the use of VariFlex by Dr. Stephen Klippenstein (Argonne National Laboratory) are gratefully acknowledged. Sandia is a multiprogram laboratory operated by Sandia Corporation, a Lockheed Martin Company, for the National Nuclear Security Administration under Contract DE-AC04-94-AL85000.

Supporting Information Available: Measured and modeled yields of final products as a function of pressure and ethylene concentration; calculated frequencies, geometries, and energies for stationary points in the C_4H_7 system; dependence of master equation calculations on energy transfer parameter; and full RMG model for vinyl iodide/ethylene photolysis system at 523 K and 533 mbar. This material is available free of charge via the Internet at http://pubs.acs.org.

References and Notes

(1) Tsang, W.; Hampson, R. F. *J. Phys. Chem. Ref. Data* **1986**, *15*, 1087.
(2) Sakai, T. In *Pyrolysis: theory and industrial practice*; Albright, L. F., Crynes, B. L., Corcoran, W. H., Eds.; Academic Press: New York, 1983; pp 89−116.
(3) Roscoe, J. M.; Bossard, A. R.; Back, M. H. *Can. J. Chem.* **2000**, *78*, 16.
(4) Thorn, R. P.; Payne, W. A.; Stief, L. J.; Tardy, D. C. *J. Phys. Chem.* **1996**, *100*, 13594.
(5) Fahr, A.; Braun, W.; Laufer, A. H. *J. Phys. Chem.* **1993**, *97*, 1502.
(6) Fahr, A.; Laufer, A.; Klein, R.; Braun, W. *J. Phys. Chem.* **1990**, *95*, 3218.
(7) Fahr, A.; Laufer, A. H. *J. Phys. Chem.* **1990**, *94*, 726.
(8) MacFadden, K. O.; Currie, C. L. *J. Chem. Phys.* **1973**, *58*, 1213.
(9) Tickner, A. W.; LeRoy, D. J. *J. Chem. Phys.* **1951**, *19*, 1247.
(10) Sherwood, A. G.; Gunning, H. E. *J. Phys. Chem.* **1965**, *69*, 2323.
(11) Weir, N. A. *J. Chem. Soc.* **1965**, 6870.
(12) Takita, S.; Mori, Y.; Tanaka, I. *J. Phys. Chem.* **1968**, *72*, 4360.
(13) Szirovicza, L. *Int. J. Chem. Kinet.* **1985**, *17*, 117.
(14) Xie, T.; McAuley, K. B.; Hsu, J. C. C.; Bacon, D. W. *Ind. Eng. Chem. Res.* **1994**, *33*, 449.
(15) Miller, J. L. *J. Phys. Chem. A* **2004**, *108*, 2268.
(16) Shestov, A. A.; Popov, K. V.; Slagle, I. R.; Knyazev, V. D. *Chem. Phys. Lett.* **2005**, *408*, 339.
(17) Richter, H.; Howard, J. B. *Prog. Energy Combust. Sci.* **2000**, *26*, 565.
(18) Fahr, A.; Stein, S. E. *Proc. Combust. Inst.* **1989**, *22*, 1023.
(19) Shahu, M.; Yang, C.-H.; Pibel, C. D.; McIlroy, A.; Taatjes, C. A.; Halpern, J. B. *J. Chem. Phys.* **2002**, *116*, 8343.
(20) Merer, A. J.; Mulliken, R. S. *Chem. Rev.* **1969**, *69*, 639.

(21) Ervin, K. M.; Gronert, S.; Barlow, S. E.; Gilles, M. K.; Harrison, A. G.; Bierbaum, V. M.; DePuy, C. H.; Lineberger, W. C.; Ellison, G. B. *J. Am. Chem. Soc.* **1990**, *112*, 5750.

(22) Klippenstein, S. J.; Wagner, A. F.; Dunbar, R. C.; Wardlaw, D. M.; Robertson, S. H.; Miller, J. A. VARIFLEX, 2002.

(23) Miller, J. A.; Klippenstein, S. J. *J. Phys. Chem. A* **2003**, *107*, 2680.

(24) Miller, J. A.; Klippenstein, S. J.; Raffy, C. *J. Phys. Chem. A* **2002**, *106*, 4904.

(25) Curtiss, L. A.; Raghavachari, K.; Redfern, P. C.; Rassolov, V.; Pople, J. A. *J. Chem. Phys.* **1998**, *109*, 7764.

(26) Frisch, M. J.; Trucks, G. W.; Schlegel, H. B.; Scuseria, G. E.; Robb, M. A.; Cheeseman, J. R.; Montgomery, J. A., Jr.; Vreven, T.; Kudin, K. N.; Burant, J. C.; Millam, J. M.; Iyengar, S. S.; Tomasi, J.; Barone, V.; Mennucci, B.; Cossi, M.; Scalmani, G.; Rega, N.; Petersson, G. A.; Nakatsuji, H.; Hada, M.; Ehara, M.; Toyota, K.; Fukuda, R.; Hasegawa, J.; Ishida, M.; Nakajima, T.; Honda, Y.; Kitao, O.; Nakai, H.; Klene, M.; Li, X.; Knox, J. E.; Hratchian, H. P.; Cross, J. B.; Bakken, V.; Adamo, C.; Jaramillo, J.; Gomperts, R.; Stratmann, R. E.; Yazyev, O.; Austin, A. J.; Cammi, R.; Pomelli, C.; Ochterski, J. W.; Ayala, P. Y.; Morokuma, K.; Voth, G. A.; Salvador, P.; Dannenberg, J. J.; Zakrzewski, V. G.; Dapprich, S.; Daniels, A. D.; Strain, M. C.; Farkas, O.; Malick, D. K.; Rabuck, A. D.; Raghavachari, K.; Foresman, J. B.; Ortiz, J. V.; Cui, Q.; Baboul, A. G.; Clifford, S.; Cioslowski, J.; Stefanov, B. B.; Liu, G.; Liashenko, A.; Piskorz, P.; Komaromi, I.; Martin, R. L.; Fox, D. J.; Keith, T.; Al-Laham, M. A.; Peng, C. Y.; Nanayakkara, A.; Challacombe, M.; Gill, P. M. W.; Johnson, B.; Chen, W.; Wong, M. W.; Gonzalez, C.; Pople, J. A. *Gaussian 03*; Gaussian, Inc.: Wallingford, CT, 2004.

(27) Pitzer, K. S.; Gwinn, W. D. *J. Chem. Phys.* **1942**, *10*, 428.

(28) Knyazev, V. D.; Bencsura, A.; Stoliarov, S. I.; Slagle, I. R. *J. Phys. Chem.* **1996**, *100*, 11346.

(29) Song, J. Building Robust Chemical Reaction Mechanisms: Next Generation of Automatic Model Construction Software. Ph.D. Dissertation, Massachusetts Institute of Technology, Cambridge, MA, 2004; http://hdl.handle.net/1721.1/ 30058.

(30) Van Geem, K. M.; Reyniers, M. F.; Marin, G. B.; Song, J.; Green, W. H.; Matheu, D. M. *AIChE J.* **2006**, *52*, 718.

(31) Howe, P.-T.; Fahr, A. *J. Phys. Chem. A* **2003**, *107*, 9603.

(32) Benson, S. W.; Haugen, G. R. *J. Phys. Chem.* **1967**, *71*, 1735.

(33) Skinner, G. B.; Sokoloski, E. M. *J. Phys. Chem.* **1960**, *64*, 1028.

(34) Tonokura, K.; Koshi, M. *J. Phys. Chem. A* **2000**, *104*, 8456.

(35) Tonokura, K.; Marui, S.; Koshi, M. *Chem. Phys. Lett.* **1999**, *313*, 771.

(36) DeSain, J. D.; Jusinski, L. E.; Taatjes, C. A. *Phys. Chem. Chem. Phys.* **2006**, *8*, 2240.

(37) Handford-Styring, S. M.; Walker, R. W. *Phys. Chem. Chem. Phys.* **2001**, *3*, 2043.

(38) Matheu, D. M.; Green, W. H., Jr.; Grenda, J. M. *Int. J. Chem. Kinet.* **2003**, *35*, 95.

(39) Stein, S. E.; Rabinovitch, B. S. *J. Phys. Chem.* **1975**, *79*, 191.

(40) Meloni, G.; Zou, P.; Klippenstein, S. J.; Ahmed, M.; Leone, S. R.; Taatjes, C. A.; Osborn, D. L. *J. Am. Chem. Soc.* **2006**, *128*, 13559.